The transmembrane adapter SCIMP recruits tyrosine kinase Syk to phosphorylate Toll-like receptors to mediate selective inflammatory outputs

Received for publication, November 7, 2021, and in revised form, March 8, 2022 Published, Papers in Press, March 22, 2022,
https://doi.org/10.1016/j.jbc.2022.101857

Liping Liu[1], Richard M. Lucas[1], Jeffrey D. Nanson[2], Yan Li[2], Jason Whitfield[1], James E. B. Curson[1], Neeraj Tuladhar[1], Kirill Alexandrov[3], Mehdi Mobli[1,4], Matthew J. Sweet[1], Bostjan Kobe[1,2], Jennifer L. Stow[1,*], and Lin Luo[1,*]

From the [1]Institute for Molecular Bioscience (IMB) and IMB Centre for Inflammation and Disease Research, and [2]School of Chemistry and Molecular Biosciences, The University of Queensland; Brisbane, Queensland, Australia; [3]CSIRO-QUT Synthetic Biology Alliance, Centre for Agriculture and the Bioeconomy, School of Biology and Environmental Science, Queensland University of Technology, Brisbane, Queensland, Australia; [4]Centre for Advanced Imaging, University of Queensland; Brisbane, Queensland, Australia

Edited by Peter Cresswell

Innate immune signaling by Toll-like receptors (TLRs) involves receptor phosphorylation, which helps to shape and drive key inflammatory outputs, yet our understanding of the kinases and mechanisms that mediate TLR phosphorylation is incomplete. Spleen tyrosine kinase (Syk) is a nonreceptor protein tyrosine kinase, which is known to relay adaptive and innate immune signaling, including from TLRs. However, TLRs do not contain the conserved dual immunoreceptor tyrosine-based activation motifs that typically recruit Syk to many other receptors. One possibility is that the Syk-TLR association is indirect, relying on an intermediary scaffolding protein. We previously identified a role for the palmitoylated transmembrane adapter protein SCIMP in scaffolding the Src tyrosine kinase Lyn, for TLR phosphorylation, but the role of SCIMP in mediating the interaction between Syk and TLRs has not yet been investigated. Here, we show that SCIMP recruits Syk in response to lipopolysaccharide-mediated TLR4 activation. We also show that Syk contributes to the phosphorylation of SCIMP and TLR4 to enhance their binding. Further evidence pinpoints two specific phosphorylation sites in SCIMP critical for its interaction with Syk-SH2 domains in the absence of immunoreceptor tyrosine-based activation motifs. Finally, using inhibitors and primary macrophages from SCIMP$^{-/-}$ mice, we confirm a functional role for SCIMP-mediated Syk interaction in modulating TLR4 phosphorylation, signaling, and cytokine outputs. In conclusion, we identify SCIMP as a novel, immune-specific Syk scaffold, which can contribute to inflammation through selective TLR-driven inflammatory responses.

As surveillance and phagocytic cells of the innate immune system, macrophages play a pivotal role in cellular recognition of both invading pathogens and endogenous tissue damage to initiate effective host defense and maintain normal homeostasis. Pathogen and damage signatures are detected mainly through a series of pattern recognition receptors, including prototypical Toll-like receptors (TLRs), which are type I single-pass transmembrane glycoproteins expressed on the plasma membrane or on endosomal membranes (1–3). Ligand-induced tyrosine phosphorylation of the TLR cytoplasmic domains is required for the recruitment of signaling adapters and subsequent activation of downstream signaling cascades (4–7). TLR4, the archetypal member of the TLR family, is activated by bacterial lipopolysaccharide (LPS) which induces phosphorylated TLR4 to engage in homotypic interactions with the intracellular Toll/interleukin-1 receptor (TIR) domains of the downstream adapters MAL and TRAM to initiate MyD88-dependent and TRIF-dependent TLR signaling, respectively (7–9). However, neither TLRs nor these adapters possess intrinsic catalytic activity, therefore these phosphorylation events are mediated by the recruitment of tyrosine kinases (10).

Studies have implicated Src family kinases, particularly Lyn, in TLR phosphorylation (11, 12). The tyrosine kinase Syk has also been implicated in TLR4 phosphorylation and signaling (13) and in the CD14-mediated endocytosis of TLR4 (14). However, how Syk is recruited to TLR4 complexes is unresolved. A prototypical Syk recruitment mechanism relies on its SH2 domains binding to immunoreceptor tyrosine-based activation motifs (ITAMs, YxxL/Ix$_{6-12}$YxxL/I) in immunoreceptors such as T-cell receptors, B-cell receptors, and Fc receptors (15–19). Such receptors signal through ITAMs that are located on either ligand-binding receptor chain itself or associated ITAM-containing transmembrane adapters, such as DAP12 (20). After ligand stimulation, Src family kinases typically phosphorylate ITAMs on dual tyrosines, which then serve as docking sites for the dual SH2 domains of Syk. The Syk-pITAM association then results in a conformational change of Syk, which disrupts its autoinhibited structure and exposes its kinase domain to activate its enzymatic activity.

* For correspondence: Lin Luo, l.luo@imb.uq.edu.au; Jennifer L. Stow, j.stow@imb.uq.edu.au.

Activated Syk then leads to downstream propagation of signaling through interaction with a wide variety of substrates and binding partners, including Vav, PLCγ, PI3K, and SLP76/SLP65 (21, 22). As a result, it leads to various cellular responses ranging from cytoskeletal reorganization and reactive oxygen species production to cell differentiation, proliferation, and survival (23, 24). Therefore, binding of two tandem SH2 domains to targeted phosphorylated tyrosine motifs is a critical step in Syk activation for downstream signaling.

TLRs do not contain classical tandem ITAM motifs, and while TLR4 contains one tyrosine (human Y^{786}RLL and mouse Y^{784}RLL) in an ITAM-like motif, the potential need for ITAM-containing scaffolds, such as DAP12, to recruit Syk has been proposed (13, 14). Consideration must be given also to other nonconventional interactions for Syk recruitment. We recently showed that the signaling kinase ERK1/2 bypasses the need for ITAM-mediated recruitment by using the transmembrane adapter, SCIMP, as a scaffold for spatiotemporal recruitment to activated TLR4 (25). SCIMP is a TLR adapter belonging to the palmitoylated transmembrane adapter protein (pTRAP) family. It is strongly expressed in myeloid-specific cells, including bone marrow–derived dendritic cells and macrophages (11, 26). SCIMP acts as a universal adapter that tailors proinflammatory cytokine secretion in multiple TLR responses mainly by promoting TLR phosphorylation (11, 27). Like other pTRAP members, SCIMP comprises a short leaderless extracellular domain and a transmembrane domain, followed by a larger cytoplasmic tail. The intracellular region contains three tyrosine residues (Y58, Y96, and Y120) and a proline-rich domain (PRD). SCIMP is constitutively associated with the Src homology 3 domain of the Src family kinase, Lyn, through its PRD domain and, following LPS stimulation, SCIMP undergoes rapid Lyn-mediated phosphorylation to induce a unique TIR–non-TIR interaction of SCIMP with TIR domain of TLR4. This association enables Lyn to be a proximal effector for TLR4 phosphorylation, thereby driving a transient signaling response, particularly in the MAPK signaling pathways (11). Given that SCIMP functions to scaffold Lyn for TLR phosphorylation and ERK1/2 for signaling, it is also a strong candidate for Syk recruitment to TLRs for inflammatory signaling.

In the present study, we examine SCIMP as a potential binding partner for Syk downstream of activated TLR4. Specific tyrosine-binding sites in SCIMP are defined for Syk recruitment and we go on to show a role for SCIMP as a scaffold for Syk-mediated phosphorylation that enhances SCIMP-TLR4 binding and biases downstream inflammatory cytokine programs. Overall, these studies reveal SCIMP as a non-ITAM, immune-specific bridging adapter for Syk recruitment and TLR4 phosphorylation in the control of macrophage inflammatory responses.

Results

Syk kinase is a novel binding partner of SCIMP

To interrogate potential interactions of Syk and other regulators with SCIMP in the context of TLR4 complexes, a GST-tagged SCIMP cytoplasmic tail (SCIMP-T1, residues 29–150) was used for pull-downs from LPS-activated macrophage extracts. To minimize nonspecific contaminant proteins from beads, bound proteins were then eluted by PreScission protease cleavage and separated by SDS-PAGE (28). Excised bands were identified by LC/MS/MS (Table S1). In addition to some known SCIMP-binding partners including TLR4 (100 kDa), Lyn (50 kDa), ERK1/2 (42/44 kDa), and Grb2 (25 kDa), Syk was also identified at 72 kDa by two independent trypsin-digested peptides, each with over 95% confidence (Fig. 1, *A* and *B*). The binding of Syk to SCIMP was then verified by further pull-downs and by immunoprecipitations from cell extracts. Figure 1*C* shows that the SCIMP cytoplasmic tail was able to bind to Syk, as well as TLR4, Grb2, and Lyn, from LPS-activated macrophage extracts. Grb2 and Lyn are known to bind to phosphorylated Y58 and to the PRD in SCIMP-T1, respectively, but not in the GST control (11). To further examine the interaction between Syk and SCIMP in human macrophages, a human macrophage cell line (THP1) overexpressing Myc-tagged SCIMP was stimulated with LPS over a time course. Whole cell lysates were immunoprecipitated with an antibody against Myc and then immunoblotted for SCIMP-binding partners. Like Lyn, Syk associated with SCIMP even in the absence of LPS. However, LPS did induce a noticeably stronger binding of SCIMP to activated phospho-Syk (Fig. 1*D*). This suggests a possible role for phosphorylation in enhancing SCIMP–Syk complex formation. Syk is known to be recruited by an ITAM-containing adapter protein DAP12 (29) in some signaling pathways such as downstream of the TREM receptor, thus affecting TLR responses *via* signaling cross-talk. We examined whether DAP12 functions to bridge Syk to SCIMP. The results showed no interaction between SCIMP and DAP12 (Fig. S1), suggesting that DAP12 is not a component of the SCIMP–Syk complex in TLR pathways. Finally, we examined the localization of Halo-SCIMP and GFP-Syk in cotransfected, LPS-treated RAW264.7 macrophages where GFP-Syk is recruited to cell surface ruffles and colocalizes with surface Halo-SCIMP (Fig. 1, *E* and *F*). Taken together, these data show that the tyrosine kinase Syk is a novel binding partner of SCIMP in macrophages. The nature of the interaction between SCIMP and Syk was next examined.

Syk binds to two specific phosphorylation sites in SCIMP

The two tandem Src homology 2 (SH2) domains of Syk are each able to bind a motif containing a phosphotyrosine site. Mouse and human SCIMP have three conserved tyrosines, which can be probed using three phosphotyrosine probes to detect selective phosphorylation (30). RAW264.7 cell extracts were collected over a two-hour time course after ligand stimulation and were used for pull-downs. All three probes captured corresponding phosphorylated tyrosines of SCIMP in response to a range of TLR ligands (TLR2, 3, and 4), indicating different temporal patterns of phosphorylation (Fig. S2, *A–C*). The quantification of SCIMP phosphorylation at its peak time point showed a significant increase at all three sites (Fig. S2, *D–F*). Interestingly, SCIMP phosphorylation at each site was

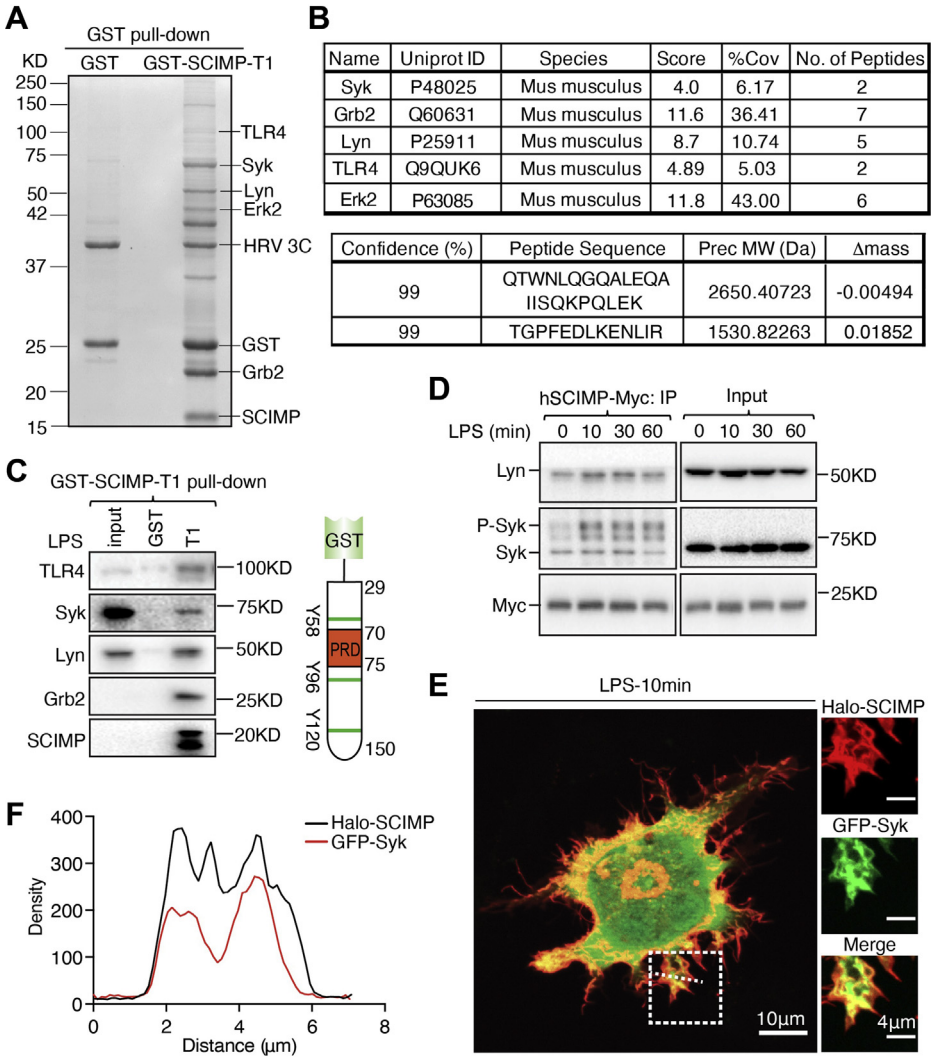

Name	Uniprot ID	Species	Score	%Cov	No. of Peptides
Syk	P48025	Mus musculus	4.0	6.17	2
Grb2	Q60631	Mus musculus	11.6	36.41	7
Lyn	P25911	Mus musculus	8.7	10.74	5
TLR4	Q9QUK6	Mus musculus	4.89	5.03	2
Erk2	P63085	Mus musculus	11.8	43.00	6

Confidence (%)	Peptide Sequence	Prec MW (Da)	Δmass
99	QTWNLQGQALEQA IISQKPQLEK	2650.40723	-0.00494
99	TGPFEDLKENLIR	1530.82263	0.01852

Figure 1. Syk is a novel binding partner of SCIMP. *A*, pull-downs from LPS-activated RAW264.7 cell extracts. GST-SCIMP-T1 was immobilized to GSH-Sepharose to capture its binding partners in macrophage lysates. Bound proteins were eluted by a protease cleavage elution (PCE) method (28) and separated by SDS–PAGE. Excised bands were identified by LC/MS/MS. *B*, list of the top hits from the LC/MS/MS analysis of GST-SCIMP-T1 pull-downs. *C*, GST-SCIMP-T1 pull-down from cell extracts of LPS activated, SCIMP-deficient RAW264.7 cells stably reconstituted with WT-V5-SCIMP. Syk and other binding partners are detected in the pull-down by immunoblotting. *D*, immunoprecipitation of myc-SCIMP-WT expressed in human PMA-differentiated THP-1 cells (56). Cells were treated with LPS over a time course and lysates made at each time point were used for IP with a Myc antibody and Syk was detected by immunoblotting. Immunoblotting of Lyn was used as a control. *E* and *F*, RAW264.7 cells cotransfected with Halo-SCIMP (*red*) and GFP-Syk (*green*). Cells were treated with Halo-549 ligand and LPS ligand for 15 min and 10 min, respectively, prior to imaging. The scale bar represents 10 μm or 4 μm. Intensity profiles of surface ruffles across the membrane (*dash white line*) is quantified for individual channels. *Panels C–E* are representative of three independent experiments.IP, immunoprecipitation; LPS, lipopolysaccharides; PMA, phorbol 12-myristate 13-acetate; Syk, Spleen tyrosine kinase.

dynamic and appeared to oscillate over time. Taken together, SCIMP is rapidly phosphorylated at Y58, Y96, and Y120 in response to multiple TLRs, which suggests these sites could all potentially be important for SCIMP–Syk interaction.

To investigate the Syk–SCIMP molecular interaction, we utilized the NH2-terminal SH2 domain (Syk-N-SH2) and COOH-terminal SH2 domain (Syk-C-SH2) of Syk as GST-tagged proteins (Fig. 2*A*) to pull-down endogenous SCIMP from primary mouse bone marrow–derived macrophages (BMMs) (Fig. 2*B*). The results from an LPS time course showed that both Syk-N-SH2 and Syk-C-SH2 have TLR4-induced binding to SCIMP, although Syk-N-SH2 is weak and Syk-C-SH2 shows greater SCIMP enrichment. Next, to identify the specific binding sites in SCIMP for the two Syk SH2 domains, CRISPR-mediated SCIMP-deficient RAW264.7 cells were reconstituted with V5-tagged SCIMP-WT or V5-tagged SCIMP-phosphorylation-deficient mutants (SCIMP-Y58F, -Y96F, and -Y120F). We used immunostaining to check that V5-tagged SCIMP-WT is expressed in a comparable fashion and in the same locations as endogenous SCIMP (Fig. S3). Extracts of these reconstituted cells were used for Syk-SH2 pull downs, and CRISPR-mediated SCIMP-deficient RAW264.7 cells were used as a negative control. We found that the binding of Syk-N-SH2 and Syk-C-SH2 to SCIMP was completely abolished in SCIMP phosphorylation-deficient mutants Y96F and Y120F, respectively, whereas the SCIMP Y58F mutation did not affect the association with Syk (Fig. 2*C*). These results suggest that phosphorylated tyrosine residue Y96 of SCIMP binds Syk-N-SH2,

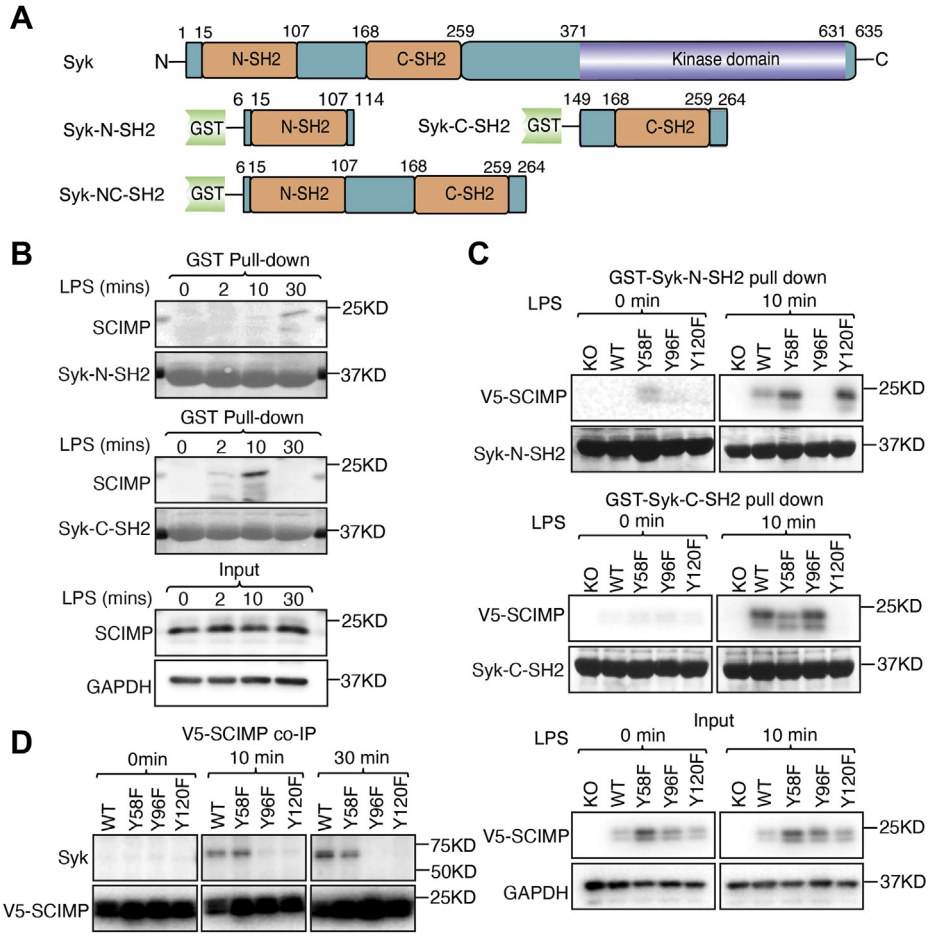

Figure 2. Syk binds to specific tyrosine residues of SCIMP *via* its dual SH2 domains. *A*, schematic diagram of Syk domains and its truncation constructs representing the two tandem SH2 domains with or without linker regions. *B*, GST-Syk-N-SH2 and Syk-C-SH2 proteins were used to pull down SCIMP from LPS-induced primary BMMs and immunoblotted with SCIMP antibody. *C*, GST-Syk-N-SH2 and Syk-C-SH2 proteins were used to pull down V5-SCIMP in SCIMP-deficient RAW264.7 cell lines reconstituted with wild type WT, Y58F, Y96F, or Y120F V5-SCIMP. *D*, coimmunoprecipitation of V5-SCIMP WT and Y58F, Y96F, or Y120F V5-SCIMP from RAW264.7 cell lysates with a V5 antibody, followed by immunoblotting for Syk. *Panels B–D* are representative of three independent experiments. BMMs, bone marrow–derived macrophages; LPS, lipopolysaccharides; SH2, Src homology domain 2; Syk, Spleen tyrosine kinase.

whereas phosphorylated Y120 docks at Syk-C-SH2. In addition, coimmunoprecipitation (co-IP) was performed in SCIMP phosphorylation-deficient mutant (Y58F, Y96F, Y120F) cell lines to further verify the SCIMP tyrosine sites for Syk interaction. Consistent with the results from pull-downs, Syk association with SCIMP was significantly reduced in Y96F and Y120F mutants, suggesting both tyrosine sites are required for the recruitment of Syk by SCIMP (Fig. 2*D*). Taken together, these results indicate that SCIMP is a scaffold for the temporal recruitment of Syk to the membrane and its two specific phosphotyrosine sites (Y96 and Y120) are responsible for binding to the tandem Syk-SH2 domains.

Syk phosphorylates TLR4 and SCIMP

The cellular function of both Lyn and Syk in TLR phosphorylation was then examined in macrophages. To firstly investigate the hierarchy of Lyn and Syk activation, RAW264.7 cells were treated with the Lyn inhibitor SU6656 over a 30 min time course, with this causing a significant reduction in Syk phosphorylation (Fig. 3*A*). This suggests that Syk lies downstream of Lyn in TLR signaling. We then investigated the role of Lyn and Syk in SCIMP and TLR4 phosphorylation. SCIMP-deleted RAW264.7 cells reconstituted with V5-SCIMP-WT were induced by LPS in the presence or absence of Lyn inhibitor (SU6656) or the Syk inhibitor (SykIV). The inhibitor SykIV was used at a concentration of 10 μM after assessing its efficacy and relative specificity with respect to SFKs (Fig. S4). Treatment with either the Lyn or Syk inhibitors attenuated SCIMP phosphorylation, as assessed by immunoprecipitation of V5-SCIMP and phospho-tyrosine blotting (Fig. 3*B*). This suggests that these two tyrosine kinases both control SCIMP activation. Next, TLR4 phosphorylation was investigated by pull-down assays. GST-TLR4-TIR recombinant proteins were generated as baits and coincubated with LPS-induced macrophage lysates for 30 min. For Syk and Lyn inhibition, each pharmacological inhibitor was added to the medium 1 h prior to LPS stimulation. GST-TLR4-TIR protein was phosphorylated by released intracellular kinases upon LPS stimulation, but the phosphorylation was significantly impaired when cells were treated with Lyn or Syk inhibitors (Fig. 3*C*). In addition, the recruitment of the SCIMP effector Erk1/2 (25) was not affected by

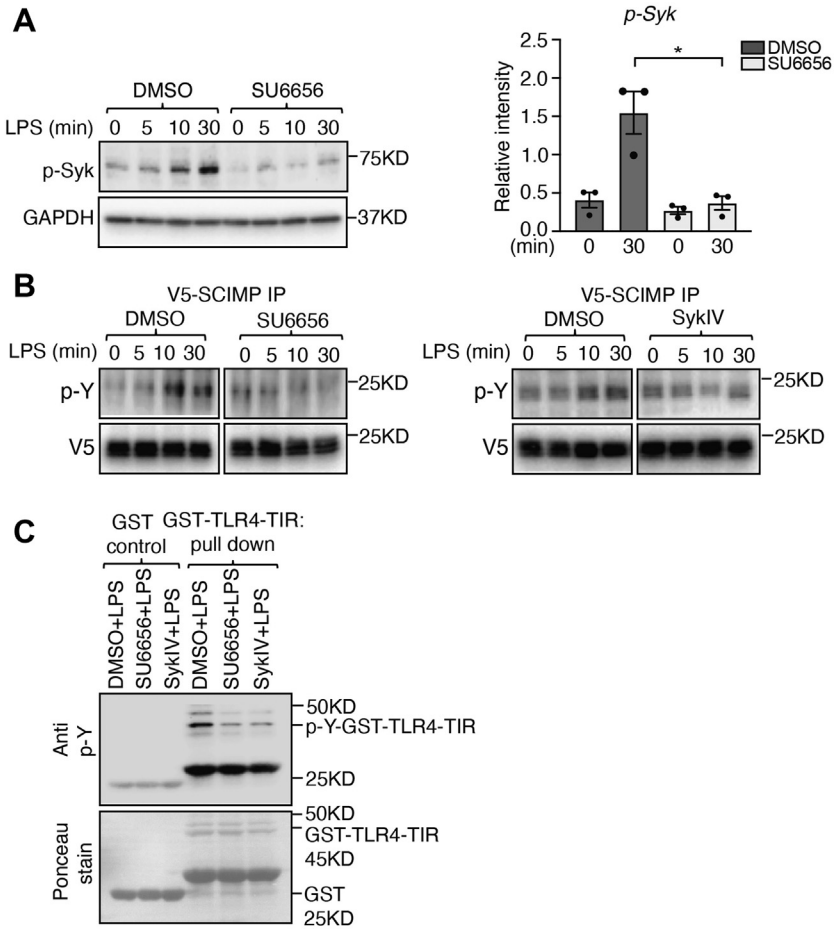

Figure 3. Syk acts downstream of Lyn for SCIMP and TLR4 phosphorylation. *A*, RAW246.7 cells were pretreated with the Lyn inhibitor SU6656 for 1 h before LPS stimulation. Phospho-Syk was detected by immunoblotting. Syk phosphorylation at the peak time point is presented as mean with SEM (n = 3) and was quantified by student's *t* test, $*p < 0.05$. *B*, V5-SCIMP was immunoprecipitated using the V5 antibody from the extracts of CRISPR-mediated SCIMP-deficient, V5-SCIMP reconstituted RAW264.7 cells. Note, the same eluate was used here (*left panel*) to probe for SCIMP phosphorylation and in Figure 5*B*. Cells were pretreated for 1 h with Lyn (SU6656) or Syk (SykIV) inhibitors before addition of LPS followed by harvesting for immunoprecipitation. *C*, GST-TLR4-TIR protein was immobilized on GSH beads and coincubated with LPS activated macrophage lysates for pull-down. Phospho-tyrosine was detected by immunoblotting in bead eluates. Data for *panels A* and *B* are representative of three independent experiments, and *panel C* is representative of two experiments. LPS, lipopolysaccharide; Syk, Spleen tyrosine kinase; TLR, Toll-like receptor.

Syk inhibition, suggesting the phosphorylation of SCIMP is not required for Erk1/2 binding (Fig. S5). Taken together, these data support Syk functioning downstream of Lyn for SCIMP and TLR4 phosphorylation.

Syk kinase activity promotes SCIMP–TLR interaction

SCIMP-TLR binding is enhanced by phosphorylation, with this modification potentially mediated by Syk and/or Lyn. At first, the interactions between SCIMP and multiple TLRs under basal, unphosphorylated conditions were examined using GST pull-downs with highly purified GST-SCIMP-T1 cytoplasmic domain as a bait on beads to capture different TIR domains in solution. The TIR domains were from purified His-tagged recombinant proteins including TLRs (TLR1, TLR2, TLR4, TLR6) and adapters (MyD88, MAL). The results revealed that TIRs from TLR1, 2, 3, and 4 directly associated with SCIMP-T1, with TLR3-TIR apparently showing particularly strong binding (Fig. S6*A*). In contrast, no interaction was observed between TLR6-TIR and SCIMP. The lack of binding of MAL or MyD88 TIRs also demonstrates the selectivity of SCIMP–TIR interactions for TLR TIRs and attests to the fidelity of this assay (Fig. S6*A*). To further characterize TIR-SCIMP binding affinity, we attempted to produce larger quantities of isolated TIRs. However, these TIR domains are notoriously difficult to produce at scale and only the TLR2-TIR was available in sufficient quantities for this analysis. The binding affinity of TLR2-TIR binding to SCIMP was then measured *via* microscale thermophoresis (MST), and dissociation constants (Kd) of 1.7 μM was detected (Fig. S6*B*). This confirms the direct interaction of this TLR/SCIMP pair but suggests they form a weak interaction *in vitro* and in the absence of protein phosphorylation within a micromolar range. Overall, these experiments show that SCIMP has a weak but direct binding to a range of TLR TIR domains under *in vitro* conditions.

In a cellular context, protein–protein interactions are often influenced by posttranslational modifications such as phosphorylation. To investigate the binding dynamic between SCIMP and TLRs in cells, co-IPs made use of SCIMP KO RAW264.7 cells stably reconstituted with V5-tagged WT SCIMP (V5-SCIMP-

WT). Cells were stimulated with the TLR2 agonist zymosan or TLR2/6 agonist FSL-1, and immunoprecipitations were performed on cell lysates using the V5 antibody. Binding of V5-SCIMP-WT with TLR2 was detected in reconstituted RAW264.7 cells upon ligand activation of the receptor (Fig. S7, *A* and *B*), in keeping with our previous finding (27). SCIMP-TLR interactions were also tested in primary BMMs treated with the TLR2 ligand Pam3CSK4 or the TLR4 ligand LPS. Activated TLR2 and TLR4 were each coimmunoprecipitated with SCIMP and these interactions peaked at 10 min, coinciding with ligand-induced tyrosine phosphorylation of SCIMP, detected with a phosphotyrosine antibody (Fig. 4, *A* and *B*). The constitutive binding of Lyn to SCIMP (Fig. 1*D* and (11)) is not affected by SCIMP phosphorylation (Fig. 4, *A* and *B*). Therefore, SCIMP phosphorylation correlates with its binding to TLRs. SCIMP phosphorylation sites were further examined using the specific phospho-probes introduced in Fig. S2. Pull-downs in BMMs made use of the three effector binding domain probes (Grb2, Csk, and SLP65) to capture SCIMP phosphorylated at Y58, Y96, and Y120. The Grb2 and Csk probes show convincing LPS-induced phosphorylation of SCIMP at Y58 and Y96. There is only mild induction of phospho-Y120 detected in BMMs using the SLP65 probe (Fig. 4*C*). Collectively, these results provide evidence for binding of SCIMP to TLR TIRs that is enhanced in cells when SCIMP is phosphorylated at all three sites.

We also examined a requirement for Syk or Lyn kinase activity to enhance SCIMP–TLR4 interactions. GST-SCIMP-T1 pulls down TLR4 from LPS-activated macrophage lysates, but this interaction was reduced in the presence of either Lyn or Syk inhibitors compared to untreated controls (Fig. 5*A*). Similarly, co-IP of TLR4 with V5-SCIMP showed peak binding at 10 min upon LPS cell stimulation and this was significantly reduced after inhibition of Lyn or Syk activity (Fig. 5*B*). These data imply that both Lyn and Syk contribute to the recruitment of SCIMP to TLR4 by controlling their phosphorylation of both proteins. Finally, to investigate whether SCIMP serves as a scaffolding protein for Syk–TLR4 interaction, we utilized purified GST-Syk-NC-SH2 for capturing TLR4 in lysates of SCIMP WT and knockout BMMs. The association between the dual SH2 Syk tail and TLR4 was reduced in SCIMP-deficient BMMs (Fig. 5*C*). Reciprocally, GST-TLR4-TIR was able to pull down Syk in WT BMMs but had reduced binding to Syk in SCIMP-deficient BMMs (Fig. 5*D*).

Taken together, these results indicate that, after being recruited to the cell surface, Syk functions to phosphorylate both SCIMP and TLR4, thus amplifying the signal output and enhancing the formation of the SCIMP–Lyn–Syk–TLR4 complex in macrophages. Pull downs in TLR adapter-deficient iBMMs showed that Syk interaction with TLR4/SCIMP was not affected by MAL, TRIF, or TRIF/TRAM deficiency (Fig. 5, *E* and *F*), suggesting that the SCIMP–Syk–TLR4 complex was formed independently of these classic TLR adapters.

Syk is an upstream kinase for SCIMP-mediated cytokine outputs in TLR pathways

Lastly, we examined LPS-induced cytokine responses in SCIMP-deficient BMMs and Syk-inhibitor treated BMMs. Consistent with our previous results (25), we found that the

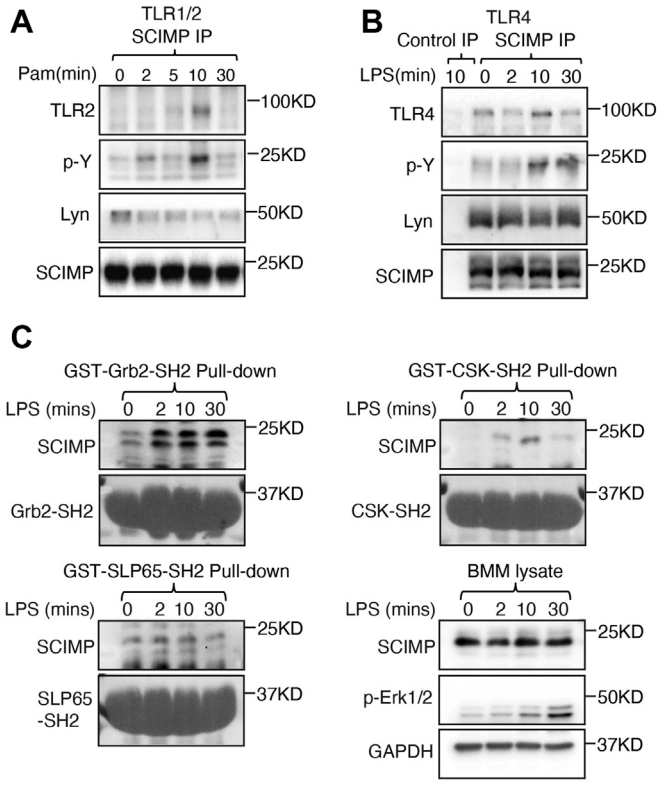

Figure 4. SCIMP-TLR interaction in macrophages. Primary BMMs were treated with the TLR2 ligand Pam3CSK4 (*A*) or the TLR4 ligand LPS (*B*), cell extracts were then used for immunoprecipitation with a SCIMP antibody, and immunoblotting detected endogenous TLR2 or TLR4, Lyn and a phospho-tyrosine antibody detected phospho-SCIMP. All data are representative of three experiments. *C*, GST-SCIMP effector-based pull-downs were performed in LPS-treated BMMs using site-specific phosphotyrosine probes (GST-Grb2-SH2, GST-Csk-SH2, and GST-SLP65-SH2) to detect SCIMP phosphorylated at sites at Y58, Y96, and Y120, respectively, shown on three separate gels. BMM lysates represent the input samples used for these pull downs immunoblotted to detect proteins of interest. BMMs, bone marrow–derived macrophages; LPS, lipopolysaccharides; TLR, Toll-like receptor.

expression of proinflammatory cytokines TNF, IL-6, and IL-12p40 was significantly decreased in SCIMP-deficient BMMs in response to LPS compared with control BMMs (Fig. 6*A*). In contrast, the synthesis of antiinflammatory IL-10 and chemokine CCL2 was unchanged in SCIMP-deficient BMMs. Noticeably, RT-PCR results from Syk-inhibited BMMs showed a similar but more potent profile in cytokine outputs than SCIMP-deficient BMMs. In addition to proinflammatory TNF, IL-6, and IL-12p40, antiinflammatory cytokine IL-10 and chemokine CCL2 were also apparently lower in Syk-inhibited BMMs than WT BMMs (Fig. 6*B*), consistent with a broader role for Syk in TLR4 signaling than SCIMP. Therefore, we identified an upstream kinase Syk that affects not only SCIMP phosphorylation and activation but also inflammatory responses downstream of activated TLR4 in macrophages.

Discussion

In this study, we revealed that the transmembrane adapter SCIMP serves as a scaffold for recruiting Syk to the nondual-ITAM containing immune receptor, TLR4. SCIMP was earlier

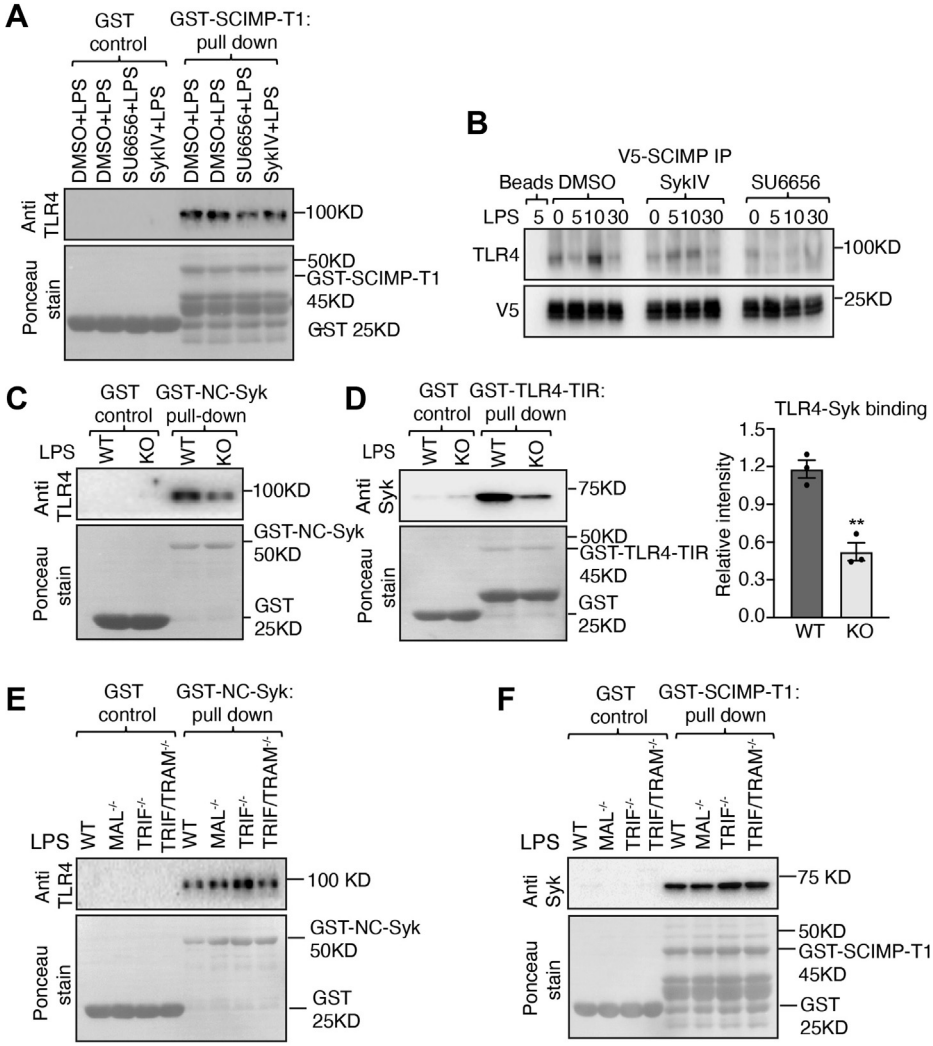

Figure 5. Phospho-tyrosine kinase activity enhances TLR4-SCIMP binding. CRISPR-mediated SCIMP-deficient RAW264.7 cells reconstituted with V5-SCIMP were untreated or pretreated with Lyn or Syk inhibitors (SU6656, SykIV) added to cells 1 h before the addition of LPS. Cell extracts were used for (*A*) pull-down by GST-SCIMP-T1; TLR4 is detected in eluates by immunoblotting and (*B*) immunoprecipitation of V5-SCIMP with a V5 antibody with TLR4 is detected by immunoblotting. Note the same eluate was used in Figure 3*B*. *C*, WT or SCIMP-deficient BMMs were treated with LPS for 30 min. GST-NC-Syk -SH2 was used as a bait to capture endogenous TLR4 detected by immunoblotting. *D*, GST-TLR4-TIR used to pull down Syk from LPS-induced WT or SCIMP-deficient BMMs; Syk detected by immunoblotting. Data are shown from three independent experiments (mean + SEM, n = 3). Quantification of TLR4-Syk binding was performed by student's *t* test, $^{**}p < 0.01$. *E*, GST-NC-Syk SH2 was used to pull down TLR4 in extracts of immortalized WT-, MAL-, TRIF-, or TRIF-/TRAM-deficient BMMs with TLR4 immunoblotted. *F*, GST-SCIMP-T1 was used to pull down Syk from extracts of immortalized WT-, MAL-, TRIF-, or TRIF-/TRAM-deficient BMMs. All data are representative of three experiments. BMMs, bone marrow–derived macrophages; LPS, lipopolysaccharides; Syk, Spleen tyrosine kinase; TLRs, Toll-like receptors.

identified as a TLR4 adapter that tailors inflammatory responses by scaffolding Lyn for TLR phosphorylation (11). Here, we identify an additional role for SCIMP in also scaffolding Syk for TLR-mediated signaling. Upon TLR activation, SCIMP is rapidly phosphorylated at all three tyrosine sites (Y58, Y96, and Y120). Our SCIMP mutagenesis studies pinpoint Y96 and Y120 as specific docking sites for binding the N-terminal and C-terminal SH2 domains of Syk, respectively. Imaging data showed that Syk colocalizes with SCIMP at known TLR signaling sites in lipid-enriched dorsal ruffles of macrophages. TLR4 failed to fully recruit Syk in *Scimp*$^{-/-}$ BMMs, suggesting a requirement of SCIMP for docking Syk to TLR4. Binding of the dual SH2 domains of Syk to the phosphorylated tyrosine sites of SCIMP at Y96 and Y120 promoted Syk activation, TLR phosphorylation, and signal amplification for inflammatory cytokine production. Therefore, we propose SCIMP is a crucial TLR transmembrane adapter for recruiting Syk and enabling TLR phosphorylation to generate a rapid inflammatory response (Fig. 7).

Ligand-induced tyrosine phosphorylation of the TLR TIR domains provides an initial mechanism for downstream adapter recruitment and intracellular signal transduction (31, 32). Syk and Src family kinase Lyn are both known to be responsible for TLR phosphorylation (11, 13). However, before the identification of SCIMP, the mechanisms of how the two kinases are recruited to TLR to enable phosphorylation were unclear. Our studies have now revealed the hierarchical order of Lyn and Syk activation *via* the transmembrane TLR adapter SCIMP. SCIMP serves as a scaffold for the recruitment of Lyn *via* its proline rich motif (11) and here, we show that SCIMP

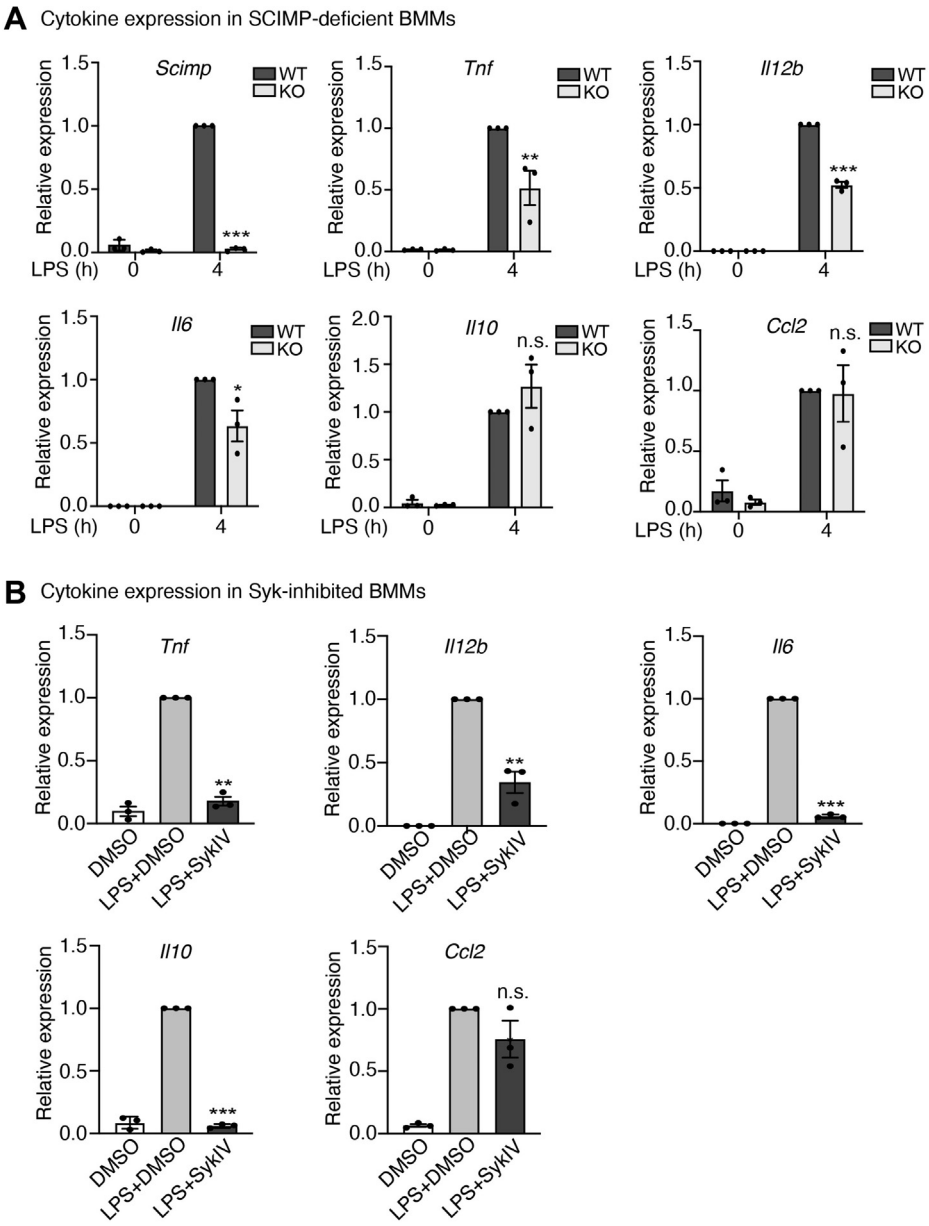

Figure 6. Regulation of TLR-induced inflammatory cytokine expression by SCIMP and Syk. *A*, BMMs were obtained from femurs and tibias of WT and SCIMP-deficient mice and treated with LPS for 4 h before analysis. mRNA levels of different types of cytokines were detected by RT-PCR and normalized relative to a house keeping gene (*Hprt*). *B*, WT BMMs were preincubated with Syk inhibitor SykIV for 1 h before LPS treatment for 4 h. Cytokines were detected at the mRNA level by RT-PCR. All data are combined from three independent experiments (n = 3) and are shown as mean + SEM. Statistical analysis was performed using student's *t* test *via* GraphPad Prism (*$p < 0.05$, **$p < 0.01$, ***$p < 0.001$). LPS, lipopolysaccharides; Syk, Spleen tyrosine kinase; TLRs, Toll-like receptors.

also scaffolds Syk *via* two phosphorylated tyrosine sites (Y96 and Y120). The Src family member Lyn phosphorylates a wide range of receptors, including TLRs (33). Unlike Syk, Lyn comprises a Src homology 3 domain, an SH2 domain followed by a C-terminal kinase domain. In its inactive state, Lyn is phosphorylated at its C-terminus by Csk enzyme, which creates a binding site for its own SH2 domain and thus holds its structure in a closed conformation. Upon ligand stimulation, dephosphorylation of the C-terminal tyrosine is catalyzed by phosphatases like CD45, allowing Lyn to be activated and recruited to membrane receptors (34, 35). Our studies showed that Lyn is the upstream kinase for both SCIMP phosphorylation and Syk phosphorylation downstream of TLR activation. Therefore, we uncover SCIMP as a missing piece in a long-standing question about how TLR4 phosphorylation is orchestrated.

Typically, Syk is recruited to immunoreceptors including B-cell receptor, T-cell receptor, and Fc receptor, through binding to two appropriately spaced phospho-tyrosines within their ITAM motifs (15–19). In the absence of conventional dual ITAM sequences in TLR4, we show that SCIMP acts as a scaffold to recruit Syk to TLR4. However, SCIMP also does not contain phospho-tyrosine sites in an ITAM configuration. Instead, we showed that Y96 and Y120 of SCIMP provide two

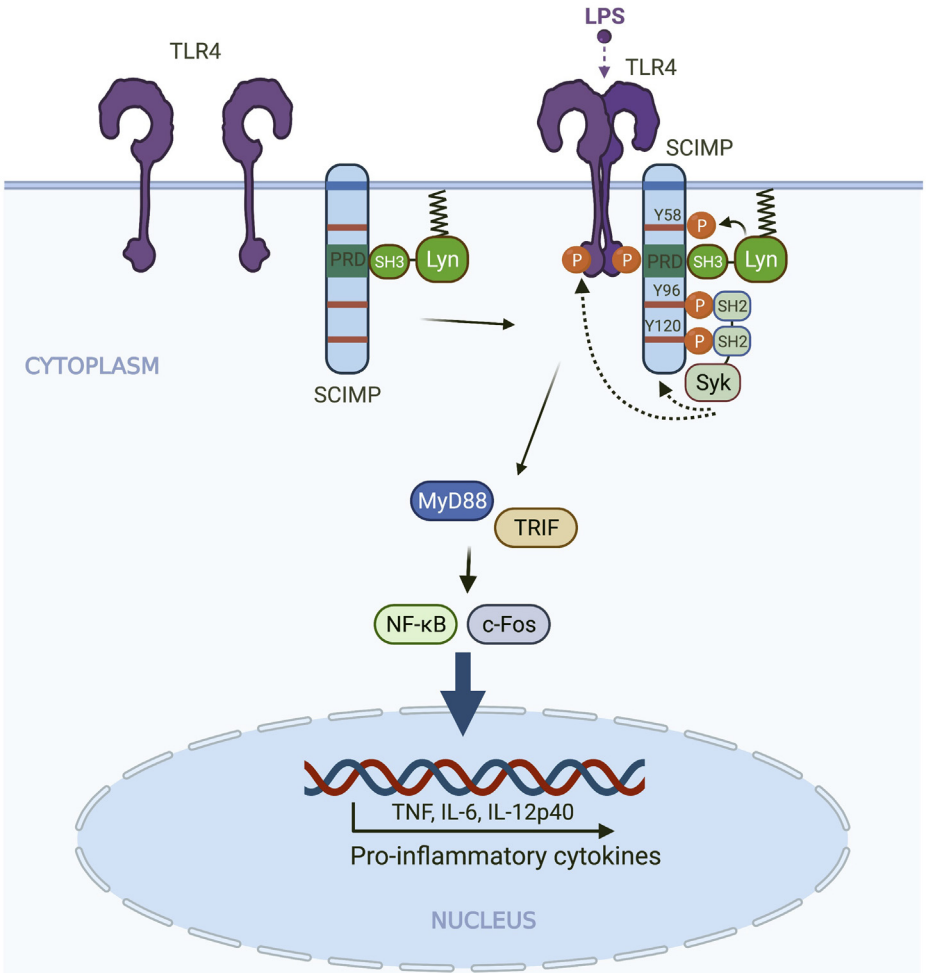

Figure 7. Model of Syk recruitment by SCIMP to TLRs. The transmembrane adapter SCIMP constitutively binds Lyn *via* a PRD-SH3 interaction. Upon ligand activation of TLR4, activated Lyn kinase phosphorylates SCIMP at three tyrosine sites. The Y96 and Y120 residues then function as two docking sites for the tandem SH2 domains of Syk, which triggers a conformational change of Syk to expose its kinase domain for amplifying SCIMP and TLR4 phosphorylation and enhancing their interaction. SCIMP-scaffolded Syk helps to propagate TLR4 signal transduction to drive proinflammatory cytokine secretion. Syk, Spleen tyrosine kinase; TLRs, Toll-like receptors; SH2, Src homology 2.

docking sites for bridging Syk, *via* SH2 domains, to the SCIMP–TLR4 complex, but these tyrosines do not have the conventional flanking residues of ITAMs. Other unconventional ITAM-like motifs that do not conform precisely to the consensus are known to bind Syk, including one in TLR4 (13) and another in Dectin-1 (36). Syk is recruited to Dectin-1, a type II transmembrane receptor of the C-type lectin family that plays an important role in antifungal innate immunity (36, 37). Only the membrane-proximal tyrosine in the Dectin-1 tail has a conventional ITAM YxxL motif, with a membrane-distal tyrosine ITAM-like motif configured as YxxxL instead. Reports proposed that the two SH2 domains of Syk can bind to two phospho-tyrosines on appropriately dimerized Dectin-1 molecules (37, 38). This model suggests that the structure of Syk has significant flexibility enabling it to bind to phosphorylated motifs with a broad range of spacing between the dual phosphorylated tyrosine residues. This also raises the issue of stoichiometry of the SCIMP–Syk complex, which remains unclear. It may be that a single Syk bridges both phosphotyrosines on one or multiple SCIMP molecules, particularly in the context of SCIMP–Syk complexes clustered with TLRs in signaling domains. Whether SCIMP also functions to scaffold and bridge Syk between different TLRs or between TLRs and Dectin-1 remains to be investigated and this is of particular interest since SCIMP is also an adapter for Dectin-1 (26).

In macrophages, we showed that the interaction between SCIMP and TLR4 in cells is enhanced by Syk kinase activity. Our results from binding assays using unphosphorylated purified proteins confirmed the direct TIR–non-TIR interaction of SCIMP with the TIR domains of several, but not all, TLRs, although the *in vitro* binding affinity remains relatively weak (~2 μM). Besides TLR4, many other TLRs including TLR1, TLR2, and TLR3 were also able to directly associate with SCIMP but no interaction was detected with other TIR-containing TLR adapters. Interestingly, no interaction was observed between SCIMP and TLR6, which is possibly due to the involvement of a unique dimeric interface for TLR6 hetero-dimerization that is not present in other TLRs (39). The direct association of SCIMP with multiple TLRs provides the foundation for SCIMP to act as a transmembrane signaling

and kinase scaffold for TLRs. In the context of cellular interactions, we confirmed here that SCIMP association with different TLRs is cell activation dependent and, for TLR2 and 4, coincides with phosphorylation of the SCIMP. Lyn and Syk kinase activities are required to stabilize the association of the TLR4–SCIMP–Lyn–Syk complex. Once the kinase activities of Lyn and Syk were inhibited, we found that SCIMP binding to TLR4 in cell lysates was significantly reduced. Consistently, Syk-TLR4 binding was also impaired in SCIMP-deficient macrophages, suggesting that SCIMP functions as a scaffold for the recruitment of Syk to TLR4. These results provide evidence that Syk activity and the scaffolding role of SCIMP are both involved in TLR phosphorylation and ensuing signaling and transcriptional cascades. To note, the reduced, but not fully abolished, Syk binding to TLR4 in SCIMP KO cells indicates that SCIMP may not be the only scaffolding protein mediating the Syk–TLR4 interaction. Aside from SCIMP, other pTRAP family members share similar binding domains (40); LAT, for instance, also contains multiple tyrosine sites which could potentially serve as docking sites for scaffolding Syk, but this remains to be formally tested.

The role of Syk in TLR signaling is controversial (22). On one hand, some studies (13, 41, 42) show that Syk kinase activity has a positive role in TLR signaling, including in myeloid cells. However, other studies also show Syk may negatively regulate TLR signaling in response to ligand activation (43) or activation *via* CD11b-TLR crosstalk (44). Signaling generated by LPS/TLR4 is modulated by multiple adapters and kinases to drive transcriptional responses biased toward proinflammatory or antiinflammatory cytokines (2, 3, 7). Cytokines are crucial mediators in the orchestration of inflammatory and innate immune responses, and homeostasis is highly dependent on the balance of various cytokines (45, 46). Previously, we have shown that SCIMP strongly promotes secretion of proinflammatory cytokines (11, 25). The selective role of SCIMP in regulating the secretion of proinflammatory cytokines including TNF, IL-12p40, and IL-6, but not anti-inflammatory cytokine IL-10 or chemokine CCL2, is confirmed in this study. Notably, this contrasts with Syk's control of both proinflammatory cytokines and IL-10. This broader role of Syk could be attributed to its involvement in multiple receptor signaling cascades. We show that SCIMP-bound Syk directly amplifies TLR phosphorylation to promote downstream signaling and cytokine release. However, Syk is also reported to be a key regulator downstream of other receptors such as Dectin-1 and TREM1/2, both of which can synergistically enhance TLR signaling *via* cross-talk (47, 48). Therefore, the robust and wide-ranging cytokine production regulated by Syk may represent a collaboration from multiple signaling pathways.

Importantly, SCIMP is associated with autoimmune and chronic inflammatory conditions (49–51). Along with other tyrosine kinases, Syk has been targeted with a range of putative inhibitors in different clinical settings. Currently, the Syk inhibitor, fostamatinib, is approved for use in immune thrombocytopenia, while Syk and its additional inhibitors are being trialed in other conditions such as chronic lymphoid leukemia (52) and COVID-19 (53). The SCIMP–Lyn–Syk complex may yet prove a tractable target for modulating TLR-induced inflammation.

Experimental procedures

Antibodies and reagents

Polyclonal antibodies of mouse SCIMP were generated against its cytoplasmic domain in rabbits by the Walter and Eliza Hall Institute Antibody Facility. Primary antibodies recognizing phospho-ERK1/2 (rabbit, #4370), GAPDH (rabbit, #5174), Grb2 (rabbit, #36344S), phospho-tyrosine (rabbit, #8954), Lyn (rabbit, #2796), Syk (rabbit, #13198) were purchased from Cell Signaling Technology. Phospho-Syk (rabbit, Tyr-525, #PA540243) antibody was purchased from Thermo Fisher Scientific Australia Pty Ltd. The monoclonal anti-TLR4 (mouse, #ab22048) and TLR2 antibodies (mouse, #AB16894) were from ABCAM Australia Pty Ltd. Antibodies detecting the V5-tag (mouse, MCA1360, clone number SV5-PK1) and Myc-tag (mouse, clone number 9E10) were bought from Sigma Aldrich. All antibodies were used at a 1:1000 dilution for immunoblotting except for phospho-Syk (1:500). Anti-rabbit or anti-mouse secondary horseradish peroxidase antibodies were used at 1:10,000. The phospho-tyrosine antibody was diluted in 2.5% bovine serum albumin (BSA), and all other antibodies were diluted in 5% skim milk. For immunoprecipitations, antibodies were used at a 1:100 dilution. The TLR ligands including Pam3CSK4 (Life Research, US1506350), Poly:IC (Integrated Sciences, P9582), LPS (Sigma-Aldrich, L9764), Imiquimod (Integrated Sciences), and Zymosan (Life Technologies, Australia) were used at concentrations of 25 ng/ml, 10 μg/ml, 100 ng/ml, 20 μg/ml, and 100 μg/ml, respectively for cell stimulation. Recombinant mouse IFNγ was used for priming cells at a concentration of 10 ng/ml (R&D Systems, 485-MI-100). Pharmacological inhibitors including Src family kinase inhibitor SU6656 (Merck, #572635) and Syk inhibitor IV (BAY 61-3606, Merck, #US1574714) were used at a 10 μM concentration. Halo-549 ligand was kindly provided by Luke Lavis from Howard Hughes Medical Institute.

DNA constructs and protein expression

His-tagged TIR domains of human TLR1, TLR2, TLR3, TLR4, TLR6, MAL, and MyD88 used for *in vitro* pull-down assays were recombinantly expressed in *Escherichia coli*. TLR3 (residues 750-904), TLR4 (residues 671-820), MAL (residues 79-221), and MyD88 (residues 155-296) TIR domain constructs were expressed as previously described (54). TLR1 (residues 632-778), TLR2 (residues 636-784), and TLR6 (residues 630-796) TIR domain constructs were cloned into the pMCSG7 expression vector by ligation independent cloning (55). GST-tagged constructs, including SCIMP-T1 (residues 29-150), Grb2-SH2 (residues 60-152), Csk-SH2 (residues 82-171), and SLP65-SH2 (residues 347-454) were designed by us, and the genes were all subcloned into pGEX6p-1 vector (GE Healthcare Life Sciences). Codon-optimized mouse TLR4-TIR (residues 670-835) gene was purchased from Genscript USA and was also subcloned in to the pGEX6p-1 vector. pGEX

plasmids for GST-tagged Syk-N-SH2 (residues 6-114, #46520), Syk-C-SH2 (residues 148-264, #46519), and Syk-NC-SH2 (residues 6-264, #46521) domains were all purchased from Addgene. GFP-Syk and V5-SCIMP constructs were subcloned to pEF6/V5-His TOPO vector (Invitrogen). For the design of Halo-tagged expressible SCIMP construct, details were published previously by our lab (25).

All His- and GST-fusion proteins were expressed in *E. coli* BL21 (DE3) cells at 30 to 37 °C with shaking (200 rpm). *E. coli* was grown to reach the mid-exponential phase (A600 = 0.6–1.0), and the His-TIR fusion proteins were produced by autoinduction at 15 to 20 °C overnight, while GST-tagged proteins were expressed *via* IPTG induction at 37 °C for 4 h. After expression, cell pellets were resuspended on ice in the lysis buffer (50 mM Hepes, 500 mM NaCl, 1 mM DTT, pH 7.5) and then were disrupted by sonication or high-pressure homogenizer for two cycles with a pressure of 30 kpsi. His-tagged proteins were purified by two steps including nickel affinity and gel-filtration chromatography. Briefly, the cell lysates were centrifuged at 20,000 rpm for 20 min at 4 °C. The supernatant was collected, loaded on a HisTrapTM FF 5 ml column (GE Healthcare), and equilibrated with lysis buffer. Unbound proteins were then removed with at least 10 column volumes of washing buffer (50 mM Hepes, 500 mM NaCl, 1 mM DTT, 50 mM imidazole, pH 7.5), and target His-tagged proteins were eluted with over a 70 ml gradient from 0% to 100% elution buffer (50 mM Hepes, 500 mM NaCl, 1 mM DTT, 350 mM imidazole, pH 7.5). Eluted proteins of interest were further purified on a Superdex 75 26/600 column (GE Healthcare), pre-equilibrated with the gel filtration buffer (10 mM Hepes, 150 mM NaCl, 1 mM DTT, pH 7.5). For GST-tagged proteins, cell lysates were captured by GSH-Sepharose beads and were directly used as bait for pull-downs, with no need to elute those proteins from beads.

Cell culture and transfection

BMMs were obtained as previously described (11). Briefly, BMMs were derived from femurs and tibias from WT C57B1/6 mice or SCIMP KO mice (6- to 12-week-old) and cultured in complete medium (RPMI 1640 medium supplemented with 2 mM L-glutamine, 10% fetal bovine serum, 50 U/ml penicillin, 50 μg/ml streptomycin). For the first 7 days, colony stimulating factor 1 (CSF-1, 10,000 U/ml) was added to the medium for BMM differentiation with a change to fresh medium and CSF-1 on day 5, thereafter, cells were used for experiments. Lentivirally transduced human THP-1 cells that express SCIMP-Myc in a doxycycline-inducible fashion have previously been described (56). The monocyte-like THP1 cells were cultured in RPMI 1640 medium supplemented with 2 mM L-glutamine, 10% fetal bovine serum, 50 U/ml penicillin, 50 μg/ml streptomycin, 10 mM Hepes, and 1 mM sodium pyruvate. The phorbol 12-myristate 13-acetate was added at a final concentration of 30 ng/ml to differentiate THP1 cells to macrophage-like cells for 48 h. 100 ng/ml of doxycycline was used to induce THP1 for 14 h before experiments for SCIMP overexpression. Immortalized BMMs were cultured in the same medium as primary BMM, without the addition of CSF-1. The macrophage-like RAW264.7 cell line was used and maintained in RPMI 1640 with 2 mM L-glutamine and 10% fetal bovine serum. Stably transfected cell lines of RAW264.7 expressing V5-SCIMP or SCIMP mutants (Y58F, Y96F, Y120F) were originally generated by electroporation and placed under selection with 2 μg/ml of blasticidin.

For imaging, transient transfection of RAW264.7 macrophages was performed using lipofectamine 2000 (Thermo Fisher Scientific). Briefly, cells were seeded on coverslips in 24-well plates (0.1×10^6 cells/500 μl complete medium) overnight. 50 μl serum-free medium with 2 μl of Lipofectamine 2000 reagent was incubated at RT for 5 min. 0.8 μg total DNA was added to 50 μl serum-free medium and then mixed with transfection reagent for 20 min at RT. Cells were changed into 400 μl serum-free medium, and 100 μl of transfection mixture was added for 3 h. After transfection, cells were cultured in complete medium overnight for further experiments.

uHPLC/MS MS/MS, mass spectrometry, and protein identification

LC/MS/MS analysis to detect SCIMP-binding partners in cells was described in our previously published paper (11). Briefly, the tryptic peptide extracts pulled down by GST-SCIMP-T1 baits from LPS-activated RAW264.7 macrophages were analyzed by microflow HPLC/MS MS/MS on an Eksigent, Ekspert nano LC400 uHPLC (SCIEX) coupled to a Triple TOF 6600 mass spectrometer (SCIEX) equipped with a micro Duo IonSpray, ion source. Five microliters of each extract was injected into a 5 mm × 300 μm, C18 3 μm trap column (SGE) for 6 min at 10 μl/min. The trapped tryptic peptide extracts were then washed onto the analytical 300 μm × 150 mm Zorbax 300SB-C18 3.5 μm column (Agilent Technologies) at 3 μl/min and a column temperature of 45 °C. Linear gradients of 2 to 25% solvent B over 60 min at 3 μl/min flow rate, followed by a steeper gradient from 25% to 35% solvent B in 13 min, then 35% to 80% solvent B in 2 min were used for peptide elution. The gradient was then returned to 2% solvent B for equilibration prior to the next sample injection. Solvent A consisted of 0.1% formic acid in water and solvent B contained 0.1% formic acid in acetonitrile. The micro ionspray voltage was set to 5500 V, declustering potential 80 V, curtain gas flow 25, nebulizer gas 1 (GS1) 15, heater gas 2 (GS2) 30 and interface heater at 150 °C. The mass spectrometer acquired 250 ms full scan TOF-MS data followed by up to 30, 50 ms full scan product ion data, with a rolling collision energy, in an Information Dependant Acquisition, IDA, scan mode. Full scan TOFMS data was acquired over the mass range m/z 350 to 2000 and for product ion ms/ms, m/z 100 to 1500. Ions observed in the TOF-MS scan exceeding a threshold of 150 counts and a charge state of +2 to +5 were set to trigger the acquisition of product ion, ms/ms spectra of the resultant 30 most intense ions. The data was acquired and processed using Analyst TF 1.7 software (ABSCIEX). Protein identification was carried out using Protein Pilot 5.0 for database searching. Details of mass spectrometry search parameters are listed in Table S2.

Fluorescence imaging

For SCIMP-Syk colocalization assay, RAW264.7 cells were plated at 0.2 × 10^6 cells/ml on 5 mm coverslips. Halo-SCIMP and GFP-Syk were transiently cotransfected into these cells using lipofectamine 2000. After overnight incubation, the cells were treated with 100 ng/ml of LPS and 10 nM of Halo-549 ligands for 10 and 15 min, respectively, before fixation in 4% paraformaldehyde for 1 h. After washing with PBS, coverslips were mounted on microscope slides using ProLong Diamond mountant (Thermo Fisher Scientific). Imaging was performed with an Axio Imager M2 with Apotome.

For the localization of overexpressed and endogenous SCIMP assay, SCIMP-depleted RAW264.7 macrophages stably reexpressing SCIMP-V5 or WT RAW264.7 macrophages were grown on 5 mm coverslips in RPMI medium containing IFNγ for 16 h. Cells were fixed in 4% PFA for 1 h, permeabilized with 0.1% Triton X-100 for 5 min, and incubated with anti-SCIMP primary antibody diluted 1:500 in 0.5% BSA/PBS for 1 h at room temperature. Cells were washed in 0.5% BSA/PBS and incubated with Alexa Fluor 488 secondary antibody diluted 1:400 in 0.5% BSA/PBS with Rhodamine Phalloidin (R415) and DAPI for 1 h at room temperature. Coverslips were mounted on microscope slides using ProLong Diamond mountant (Thermo Fisher Scientific). 5 phase shift images were acquired on an Axio Imager M2 with Apotome.2 fitted with a Plan Neofluar 40x NA 1.3 oil objective using Zeiss Zen 2 software with a Zeiss Axiocam 506 camera.

Generation of CRISPR-mediated SCIMP-deficient cells and reconstituted V5-SCIMP cells

The details of CRISPR/Cas9-mediated SCIMP gene knockout in RAW264.7 macrophages were described in our previously published paper (11). Briefly, S.p. Cas9 Nuclease 3NLS (Cat No. 1074181), Alt-R CRISPR crRNA targeting SCIMP (50 -GCCACCT GCAGACACAGTAC-30), and Alt-R CRISPR tracrRNA (Cat No. 1072532) were purchased from Integrated DNA Technologies. Those RNAs were then transfected to RAW264.7 cells by using CRISPRMAX transfection reagent from Thermo-Fisher (Cat No. CMAX00003). After G418 selection for 3 days, colonies were tested for SCIMP knockout by Western blot. To generate V5-SCIMP reconstituted macrophages, the V5-SCIMP was introduced by electroporation into SCIMP-KO RAW264.7 cells and the stable cell line was selected using blasticidin.

Direct SCIMP-TLR TIR in vitro interaction assays, pull-down assays, and immunoprecipitations

Direct SCIMP-TLR TIR *in vitro* interaction assays were performed using purified GST-hSCIMP T1 bound to immobilized GSH-Sepharose beads as 'bait' to capture purified His-tagged TIR domains from TLRs 1/2/3/4/6, MyD88, and MAL as 'prey', which were individually coincubated in micro spin columns (#27-3565-01; GE Healthcare) on a roller at 4 °C for 2 h before elution. For other GST–pull-down assays, the detailed processes were described previously (27). Briefly, GST-tagged purified bait proteins immobilized on GSH-Sepharose beads were incubated with cells extracts. Cells were plated in P30 plates at a density of 1 × 10^6 cells/ml and cultured overnight before ligand treatment. Where kinase inhibitors were used, they were preincubated with cells 1 h prior to ligand stimulation. Cells were then harvested and lysed in lysis buffer A (25 mM Tris, pH 7.4, 150 mM NaCl, 1% NP-40, 1% Triton 100, 5% glycerol, with addition of cOmplete Mini EDTA-free protease inhibitor cocktail tablets (Sigma-Adrich) and PhosSTOP tablets (Roche Applied Science)). Supernatants were then collected by high-speed centrifugation and incubated with GST-bait protein-bound beads on a roller at 4 °C for 2 h. Fifty microliter of cell lysate supernatants were kept as input samples. After incubation, samples were centrifuged at 500*g* for 1 min to remove unbound proteins, and beads were then washed 4 times with 500 μl of ice-cold lysis buffer. Finally, bound proteins were heated at 95 °C for 10 min and eluted in 2 X SDS-PAGE sample buffer for Western blot analysis.

Immunoprecipitations were performed with cells plated in P30 tissue culture plates and harvested in the lysis buffer A and lysed by successive passage through 27-gauge needles. Supernatants were collected after centrifugation at 17,000*g* for 15 min and were added to micro spin columns to incubate with antibody-bound protein G beads (5 μl of antibodies bound to 20 μl beads) at 4 °C for at least 1 h. Beads were then washed with ice-cold lysis buffer A three times before elution with 2 X SDS-PAGE sample buffer and heating and running on SDS-PAGE gels for Western blotting.

In-vitro binding affinity

MST were used to quantify the binding affinity of the interaction between the TLR2 TIR domain and SCIMP cytoplasmic domain. Purified GFP-hSCIMP-His protein was used for florescence measurement at a constant concentration of 600 nM. Purified His-hTLR2 TIR protein were diluted at a series of concentrations (100, 50, 30, 20, 15, 10, 7.5, 5, 2, 1, 0.5, 0.2, 0.1, 0.01, 0 μM) for mixing with GFP-hSCIMP-His for 15 min at RT before loading into MonolithTM NT.115 hydrophilic capillaries. BSA and GST proteins were SCIMP-unbound proteins and were used as negative controls. The buffer used for diluting protein was 10 mM Hepes, 150 mM NaCl, 0.05% Tween-20, pH 7.5. The LED power of the instrument was 50% and the MST power was 80%. Binding curves were obtained at 37 °C and fitted using sigmoidal nonlinear regression. The Kd values were calculated by fitting the T-jump signal.

Cytokine gene expression analysis via RT-PCR

Cytokine mRNA levels were measured by RT-PCR, as previously described (27). Briefly, BMMs were plated into 6-well plates at 1 × 10^6 cells/well for overnight before stimulation with LPS for 4 h. Then, cells were washed in chilled PBS before lysis in RLT buffer followed by mRNA extraction using kits (Qiagen, Chadstone Centre) according to the manufacturer's guidelines. Extracted mRNA was adjusted to the same concentration, and 1 μg of mRNA was converted to first-strand cDNA using kit containing Superscript III and oligo dT primers (Invitrogen). Gene expression was then quantified by SYBR green (Applied Biosystems) RT-qPCR (15 s at 95 °C and

1 min at 60 °C for 45 cycles) using the Applied Biosystems ViiA7 Real Time PCR system (Life technologies). *Hprt* was used as a control for normalization.

Statistics

All datasets subjected to statistical analysis were compiled from three independent experiments (n = 3). All data are presented as arithmetic mean ± standard error of the mean. Student's *t* test was used for direct comparison of a single experimental variable. In all statistical analyses, a p value <0.05 was considered statistically significant and descriptions of individual p values calculated for each experimental comparison are stated in the respective figure legends. Statistics were calculated using GraphPad Prism 9.

Data availability

All data are contained within the article.

Supporting information—This article contains supporting information.

Acknowledgments—Our thanks to Tatiana Khromykh for help with molecular cloning, William Sturgess (SCMB, UQ) for cloning human TLR-TIR constructs, and Darren Brown for expert technical support. Our sincere thanks to Tomas Brdicka, Institute of Molecular Genetics AS CR, Prague, CZ for kindly providing human SCIMP constructs and reagents. We also thank Dr Alun Jones for expert support in the IMB Mass Spectroscopy facility. Cell imaging was performed at IMB in the Cancer Ultrastructure and Function Facility funded by the Australian Cancer Research Foundation. All animal studies were approved by The University of Queensland Animal Ethics Committee (AEC Approval number: IMB/026/19).

Author contributions—L. Liu, J. L. S., and L. Luo, conceptualization; J. D. N., Y. L., J. W., J. E. B. C., M. M., M. J. S., B. K., K. A. reagents; L. Liu, R. M. L., J. W., N. T., M. M., B. K., K. A., and L. Luo, methodology; L. Liu., R. M. L., J. W., M. M., and L. Luo, investigation; J. L. S. and L. Luo, funding acquisition; J. L. S. and L. Luo, supervision; L. Liu and L. Luo writing–original draft; L. Liu., M. J. S., J. L. S., and L. Luo. writing–review & editing.

Funding and additional information—This work was supported by Australian Research Council DECRA Fellowship DE180100524 (L. Luo.), National Health and Medical Research Council of Australia Investigator Grant APP1176209 and Project grant APP1138723 (J. L. S.), National Health and Medical Research Council of Australia Project Grant APP1159106 (L. Luo and J. L. S), and National Health and Medical Research Council of Australia Investigator Grant APP1194406 (M. J. S.).

Conflict of interest—The authors declare that they have no conflicts of interest with the contents of this article.

Abbreviations—The abbreviations used are: BSA, bovine serum albumin; BMM, bone marrow–derived macrophages; co-IP, coimmunoprecipitation; CSF-1, colony stimulating factor 1; ITAM, immunoreceptor tyrosine-based activation motif; LPS, lipopolysaccharide; MST, microscale thermophoresis; PRD, proline-rich domain; pTRAP, palmitoylated transmembrane adapter protein; SH2, Src homology 2 domain; Syk, Spleen tyrosine kinase; TLR, Toll-like receptor; TIR, Toll/interleukin-1 receptor domain.

References

1. Gordon, S. (2002) Pattern recognition receptors: Doubling up for the innate immune response. *Cell* **111**, 927–930
2. Akira, S., and Takeda, K. (2004) Toll-like receptor signalling. *Nat. Rev. Immunol.* **4**, 499–511
3. Fitzgerald, K. A., and Kagan, J. C. (2020) Toll-like receptors and the control of immunity. *Cell* **180**, 1044–1066
4. Medvedev, A. E., Piao, W., Shoenfelt, J., Rhee, S. H., Chen, H., Basu, S., Wahl, L. M., Fenton, M. J., and Vogel, S. N. (2007) Role of TLR4 tyrosine phosphorylation in signal transduction and endotoxin tolerance. *J. Biol. Chem.* **282**, 16042–16053
5. Sabroe, I., Read, R. C., Whyte, M. K., Dockrell, D. H., Vogel, S. N., and Dower, S. K. (2003) Toll-like receptors in health and disease: Complex questions remain. *J. Immunol.* **171**, 1630–1635
6. Verstak, B., Stack, J., Ve, T., Mangan, M., Hjerrild, K., Jeon, J., Stahl, R., Latz, E., Gay, N., Kobe, B., Bowie, A. G., and Mansell, A. (2014) The TLR signaling adaptor TRAM interacts with TRAF6 to mediate activation of the inflammatory response by TLR4. *J. Leukoc. Biol.* **96**, 427–436
7. Gay, N. J., Symmons, M. F., Gangloff, M., and Bryant, C. E. (2014) Assembly and localization of Toll-like receptor signalling complexes. *Nat. Rev. Immunol.* **14**, 546–558
8. Rossol, M., Heine, H., Meusch, U., Quandt, D., Klein, C., Sweet, M. J., and Hauschildt, S. (2011) LPS-induced cytokine production in human monocytes and macrophages. *Crit. Rev. Immunol.* **31**, 379–446
9. Xiong, Y., Song, C., Snyder, G. A., Sundberg, E. J., and Medvedev, A. E. (2012) R753Q polymorphism inhibits Toll-like receptor (TLR) 2 tyrosine phosphorylation, dimerization with TLR6, and recruitment of myeloid differentiation primary response protein 88. *J. Biol. Chem.* **287**, 38327–38337
10. Chattopadhyay, S., and Sen, G. C. (2014) Tyrosine phosphorylation in Toll-like receptor signaling. *Cytokine Growth Factor Rev.* **25**, 533–541
11. Luo, L., Bokil, N. J., Wall, A. A., Kapetanovic, R., Lansdaal, N. M., Marceline, F., Burgess, B. J., Tong, S. J., Guo, Z., Alexandrov, K., Ross, I. L., Hibbs, M. L., Stow, J. L., and Sweet, M. J. (2017) SCIMP is a transmembrane non-TIR TLR adaptor that promotes proinflammatory cytokine production from macrophages. *Nat. Commun.* **8**, 14133
12. Mitchell, J., Kim, S. J., Seelmann, A., Veit, B., Shepard, B., Im, E., and Rhee, S. H. (2018) Src family kinase tyrosine phosphorylates Toll-like receptor 4 to dissociate MyD88 and Mal/Tirap, suppressing LPS-induced inflammatory responses. *Biochem. Pharmacol.* **147**, 119–127
13. Chaudhary, A., Fresquez, T. M., and Naranjo, M. J. (2007) Tyrosine kinase Syk associates with Toll-like receptor 4 and regulates signaling in human monocytic cells. *Immunol. Cell Biol.* **85**, 249–256
14. Zanoni, I., Ostuni, R., Marek, L. R., Barresi, S., Barbalat, R., Barton, G. M., Granucci, F., and Kagan, J. C. (2011) CD14 controls the LPS-induced endocytosis of Toll-like receptor 4. *Cell* **147**, 868–880
15. Chan, A. C., Iwashima, M., Turck, C. W., and Weiss, A. (1992) ZAP-70: A 70 kd protein-tyrosine kinase that associates with the TCR zeta chain. *Cell* **71**, 649–662
16. Stepanek, O., Draber, P., Drobek, A., Horejsi, V., and Brdicka, T. (2013) Nonredundant roles of Src-family kinases and Syk in the initiation of B-cell antigen receptor signaling. *J. Immunol.* **190**, 1807–1818
17. Heizmann, B., Reth, M., and Infantino, S. (2010) Syk is a dual-specificity kinase that self-regulates the signal output from the B-cell antigen receptor. *Proc. Natl. Acad. Sci. U. S. A.* **107**, 18563–18568
18. Sedlik, C., Orbach, D., Veron, P., Schweighoffer, E., Colucci, F., Gamberale, R., Ioan-Facsinay, A., Verbeek, S., Ricciardi-Castagnoli, P., Bonnerot, C., Tybulewicz, V. L., Di Santo, J., and Amigorena, S. (2003) A critical role for Syk protein tyrosine kinase in Fc receptor-mediated antigen presentation and induction of dendritic cell maturation. *J. Immunol.* **170**, 846–852
19. Bonnerot, C., Briken, V., Brachet, V., Lankar, D., Cassard, S., Jabri, B., and Amigorena, S. (1998) Syk protein tyrosine kinase regulates Fc receptor gamma-chain-mediated transport to lysosomes. *EMBO J.* **17**, 4606–4616

20. Mocsai, A., Humphrey, M. B., Van Ziffle, J. A., Hu, Y., Burghardt, A., Spusta, S. C., Majumdar, S., Lanier, L. L., Lowell, C. A., and Nakamura, M. C. (2004) The immunomodulatory adapter proteins DAP12 and Fc receptor gamma-chain (FcRgamma) regulate development of functional osteoclasts through the Syk tyrosine kinase. *Proc. Natl. Acad. Sci. U. S. A.* **101**, 6158–6163
21. Deng, G. M., Kyttaris, V. C., and Tsokos, G. C. (2016) Targeting syk in Autoimmune Rheumatic diseases. *Front. Immunol.* **7**, 78
22. Miller, Y. I., Choi, S. H., Wiesner, P., and Bae, Y. S. (2012) The SYK side of TLR4: Signalling mechanisms in response to LPS and minimally oxidized LDL. *Br. J. Pharmacol.* **167**, 990–999
23. Mocsai, A., Ruland, J., and Tybulewicz, V. L. (2010) The SYK tyrosine kinase: A crucial player in diverse biological functions. *Nat. Rev. Immunol.* **10**, 387–402
24. Berton, G., Mocsai, A., and Lowell, C. A. (2005) Src and syk kinases: Key regulators of phagocytic cell activation. *Trends Immunol.* **26**, 208–214
25. Lucas, R. M., Liu, L., Curson, J. E. B., Koh, Y. W. H., Tuladhar, N., Condon, N. D., Das Gupta, K., Burgener, S. S., Schroder, K., Ingley, E., Sweet, M. J., Stow, J. L., and Luo, L. (2021) SCIMP is a spatiotemporal transmembrane scaffold for Erk1/2 to direct pro-inflammatory signaling in TLR-activated macrophages. *Cell Rep.* **36**, 109662
26. Kralova, J., Fabisik, M., Pokorna, J., Skopcova, T., Malissen, B., and Brdicka, T. (2016) The transmembrane adaptor protein SCIMP facilitates sustained dectin-1 signaling in dendritic cells. *J. Biol. Chem.* **291**, 16530–16540
27. Luo, L., Curson, J. E. B., Liu, L., Wall, A. A., Tuladhar, N., Lucas, R. M., Sweet, M. J., and Stow, J. L. (2020) SCIMP is a universal Toll-like receptor adaptor in macrophages. *J. Leukoc. Biol.* **107**, 251–262
28. Luo, L., King, N. P., Yeo, J. C., Jones, A., and Stow, J. L. (2014) Single-step protease cleavage elution for identification of protein-protein interactions from GST pull-down and mass spectrometry. *Proteomics* **14**, 19–23
29. N'Diaye, E. N., Branda, C. S., Branda, S. S., Nevarez, L., Colonna, M., Lowell, C., Hamerman, J. A., and Seaman, W. E. (2009) TREM-2 (triggering receptor expressed on myeloid cells 2) is a phagocytic receptor for bacteria. *J. Cell Biol.* **184**, 215–223
30. Luo, L., Tong, S. J., Wall, A. A., Khromykh, T., Sweet, M. J., and Stow, J. L. (2017) Development of SH2 probes and pull-down assays to detect pathogen-induced, site-specific tyrosine phosphorylation of the TLR adaptor SCIMP. *Immunol. Cell Biol.* **95**, 564–570
31. Biswas, C., Rao, S., Slade, K., Hyman, D., Dersh, D., Mantegazza, A. R., Zoltick, P. W., Marks, M. S., Argon, Y., and Behrens, E. M. (2018) Tyrosine 870 of TLR9 is critical for receptor maturation rather than phosphorylation-dependent ligand-induced signaling. *PLoS One* **13**, e0200913
32. Lee, K. G., Xu, S., Kang, Z. H., Huo, J., Huang, M., Liu, D., Takeuchi, O., Akira, S., and Lam, K. P. (2012) Bruton's tyrosine kinase phosphorylates Toll-like receptor 3 to initiate antiviral response. *Proc. Natl. Acad. Sci. U. S. A.* **109**, 5791–5796
33. Sanjuan, M. A., Rao, N., Lai, K. T., Gu, Y., Sun, S., Fuchs, A., Fung-Leung, W. P., Colonna, M., and Karlsson, L. (2006) CpG-induced tyrosine phosphorylation occurs *via* a TLR9-independent mechanism and is required for cytokine secretion. *J. Cell Biol.* **172**, 1057–1068
34. Xu, Y., Harder, K. W., Huntington, N. D., Hibbs, M. L., and Tarlinton, D. M. (2005) Lyn tyrosine kinase: Accentuating the positive and the negative. *Immunity* **22**, 9–18
35. Okada, M. (2012) Regulation of the SRC family kinases by Csk. *Int. J. Biol. Sci.* **8**, 1385–1397
36. Fuller, G. L., Williams, J. A., Tomlinson, M. G., Eble, J. A., Hanna, S. L., Pohlmann, S., Suzuki-Inoue, K., Ozaki, Y., Watson, S. P., and Pearce, A. C. (2007) The C-type lectin receptors CLEC-2 and Dectin-1, but not DC-SIGN, signal *via* a novel YXXL-dependent signaling cascade. *J. Biol. Chem.* **282**, 12397–12409
37. Rogers, N. C., Slack, E. C., Edwards, A. D., Nolte, M. A., Schulz, O., Schweighoffer, E., Williams, D. L., Gordon, S., Tybulewicz, V. L., Brown, G. D., and Reis e Sousa, C. (2005) Syk-dependent cytokine induction by Dectin-1 reveals a novel pattern recognition pathway for C type lectins. *Immunity* **22**, 507–517
38. Goodridge, H. S., Wolf, A. J., and Underhill, D. M. (2009) Beta-glucan recognition by the innate immune system. *Immunol. Rev.* **230**, 38–50
39. Jang, T. H., and Park, H. H. (2014) Crystal structure of TIR domain of TLR6 reveals novel dimeric interface of TIR-TIR interaction for Toll-like receptor signaling pathway. *J. Mol. Biol.* **426**, 3305–3313
40. Curson, J. E. B., Luo, L., Sweet, M. J., and Stow, J. L. (2018) pTRAPs: Transmembrane adaptors in innate immune signaling. *J Leukoc. Biol.* https://doi.org/10.1002/JLB.2RI1117-474R
41. Lin, Y. C., Huang, D. Y., Chu, C. L., and Lin, W. W. (2010) Anti-inflammatory actions of Syk inhibitors in macrophages involve non-specific inhibition of toll-like receptors-mediated JNK signaling pathway. *Mol. Immunol.* **47**, 1569–1578
42. Zanoni, I., Tan, Y., Di Gioia, M., Springstead, J. R., and Kagan, J. C. (2017) By capturing inflammatory lipids released from dying cells, the receptor CD14 induces inflammasome-dependent phagocyte hyperactivation. *Immunity* **47**, 697–709.e693
43. Lin, Y. C., Huang, D. Y., Chu, C. L., Lin, Y. L., and Lin, W. W. (2013) The tyrosine kinase Syk differentially regulates Toll-like receptor signaling downstream of the adaptor molecules TRAF6 and TRAF3. *Sci. Signal.* **6**, ra71
44. Han, C., Jin, J., Xu, S., Liu, H., Li, N., and Cao, X. (2010) Integrin CD11b negatively regulates TLR-triggered inflammatory responses by activating Syk and promoting degradation of MyD88 and TRIF *via* Cbl-b. *Nat. Immunol.* **11**, 734–742
45. Bieghs, V., and Trautwein, C. (2013) The innate immune response during liver inflammation and metabolic disease. *Trends Immunol.* **34**, 446–452
46. Kopf, M., Bachmann, M. F., and Marsland, B. J. (2010) Averting inflammation by targeting the cytokine environment. *Nat. Rev. Drug Discov.* **9**, 703–718
47. Bouchon, A., Facchetti, F., Weigand, M. A., and Colonna, M. (2001) TREM-1 amplifies inflammation and is a crucial mediator of septic shock. *Nature* **410**, 1103–1107
48. Hamerman, J. A., Tchao, N. K., Lowell, C. A., and Lanier, L. L. (2005) Enhanced Toll-like receptor responses in the absence of signaling adaptor DAP12. *Nat. Immunol.* **6**, 579–586
49. Luo, L., Lucas, R. M., Liu, L., and Stow, J. L. (2019) Signalling, sorting and scaffolding adaptors for toll-like receptors. *J. Cell Sci.* **133**, jcs239194
50. Dozmorov, M. G., Wren, J. D., and Alarcon-Riquelme, M. E. (2014) Epigenomic elements enriched in the promoters of autoimmunity susceptibility genes. *Epigenetics* **9**, 276–285
51. Jansen, I. E., Savage, J. E., Watanabe, K., Bryois, J., Williams, D. M., Steinberg, S., Sealock, J., Karlsson, I. K., Hagg, S., Athanasiu, L., Voyle, N., Proitsi, P., Witoelar, A., Stringer, S., Aarsland, D., *et al.* (2019) Genome-wide meta-analysis identifies new loci and functional pathways influencing Alzheimer's disease risk. *Nat. Genet.* **51**, 404–413
52. Liu, D., and Mamorska-Dyga, A. (2017) Syk inhibitors in clinical development for hematological malignancies. *J. Hematol. Oncol.* **10**, 145
53. Strich, J. R., Ramos-Benitez, M. J., Randazzo, D., Stein, S. R., Babyak, A., Davey, R. T., Suffredini, A. F., Childs, R. W., and Chertow, D. S. (2021) Fostamatinib inhibits neutrophils extracellular traps induced by COVID-19 patient plasma: A potential therapeutic. *J. Infect. Dis.* **223**, 981–984
54. Ve, T., Vajjhala, P. R., Hedger, A., Croll, T., DiMaio, F., Horsefield, S., Yu, X., Lavrencic, P., Hassan, Z., Morgan, G. P., Mansell, A., Mobli, M., O'Carroll, A., Chauvin, B., Gambin, Y., *et al.* (2017) Structural basis of TIR-domain-assembly formation in MAL- and MyD88-dependent TLR4 signaling. *Nat. Struct. Mol. Biol.* **24**, 743–751
55. Stols, L., Gu, M., Dieckman, L., Raffen, R., Collart, F. R., and Donnelly, M. I. (2002) A new vector for high-throughput, ligation-independent cloning encoding a tobacco etch virus protease cleavage site. *Protein Expr. Purif.* **25**, 8–15
56. Curson, J. E., Luo, L., Liu, L., Burgess, B. J., Bokil, N. J., Wall, A. A., Brdicka, T., Kapetanovic, R., Stow, J. L., and Sweet, M. J. (2022) An alternative downstream translation start site in the non-TIR adaptor Scimp enables selective amplification of CpG DNA responses in mouse macrophages. *Immunol Cell Biol.* **100**, 267–284